**SAINS TANAH – Journal of Soil Science and Agroclimatology**

Journal homepage: http://jurnal.uns.ac.id/tanah

# Distribution of nickel (Ni) in peatland situated alongside mineral soil derived from ultrabasic rocks

**Heru Bagus Pulunggono[1]*, Moh Zulfajrin[2], Fuadi Irsan[3]**

[1] Department of Soil Science and Land Resources, Faculty of Agriculture, IPB University, Indonesia
[2] Graduated Program of Soil Science and Land Resources Department, Faculty of Agriculture, IPB University, Indonesia
[3] Indonesian Agency for Agricultural Research and Development (BPTP) South Sumatera, Ministry of Agriculture, Palembang, Indonesia

**ARTICLE INFO**

**Keywords**:
Nickel characteristics
Peat
Ultrabasic mineral soil
Morowali

Article history
*Submitted: 2020-11-05*
*Accepted: 2021-06-05*
*Available online: 2021-06-30*
*Published regularly: June 2021*

* *Corresponding Author*
*Email address:*
*heruipb@yahoo.co.id*

**ABSTRACT**

Detailed studies of Ni distribution in peat that is influenced by Ni-rich soil derived from ultrabasic rocks are still limited. The objective of this study was to reveal the characteristics of Ni in peat from Morowali (Central Sulawesi Province, Indonesia) at several depths and distances from the boundary of the ultrabasic mineral soil. Peat was sampled from depths of 0–30, 30–60, and 60–90 cm at distances of 100, 200, 300, 400, 500, and 600 m from the border of the ultrabasic mineral soil in March 2018. Ni characteristics were examined through their total, exchangeable, water-soluble, and adsorbed distributions. The relationships between Ni and some peat chemical properties such as pH; cation exchange capacity; macronutrient contents of K, Ca, and Mg; and micronutrient contents of Fe, Cu and Zn were also observed. The high Ni content in peat at the study transect is caused by an accumulation of Ni transported from elevated areas of mineral soil. Most Ni in peat is bonded to the soil organic exchange complexes. Accumulation of the mineral soil fraction in the peat surface is indicated at distances of 100–400 meters from the ultrabasic mineral soil. Ni distribution in peat at the study transect is mainly governed by a combination of Fe, pH, organic material, water content, peat depth, and distance from ultrabasic mineral soil.

**How to Cite**: Pulunggono, H. B., Zulfajrin, M., & Irsan, F. (2021). Distribution of nickel (Ni) in peatland situated alongside mineral soil derived from ultrabasic rocks. Sains Tanah Journal of Soil Science and Agroclimatology, 18(1): 15-26. https://dx.doi.org/10.20961/stjssa.v18i1.45417

## 1. Introduction

There are numerous studies of nutrient distributions in tropical peat (Pulunggono et al., 2019; Watanabe et al., 2013). However, almost all of these studies focused on the chemical properties of peat overlying mineral soil that is derived from fluviatile sediments of felsic–andesitic rock areas. Fu et al. (2014) and Ritung et al. (2019) reported that the peat in Morowali, Central Sulawesi, developed in a backswamp area consisting of an ultrabasic formation. Weathering from this type of rock formed a laterite soil containing high amounts of Ni (Tupaz et al., 2020; Zhang et al., 2020). This soil has long been cultivated by local farmers for cash crops and oil palm plantation companies.

Despite its status as an essential nutrient for the growth and development of several higher plants (Siqueira Freitas et al., 2018), elevated Ni concentration in soil adversely affects plants (Jiang et al., 2019), animals, and humans (Das et al., 2019; Genchi et al., 2020). Accumulation of Ni in plant tissue is detrimental to agricultural product quality, leading to the disruption of chemical and biological activities in the human body (Olafisoye et al., 2020; Sreekanth et al., 2013). Tropical peat has high acidity (Abat et al., 2012; Sangok et al., 2020) and low nutrient status (Watanabe et al., 2013). The decreasing soil pH in peat could increase Ni availability (Lin et al., 2015; Ma et al., 2013), which exceeds normal concentrations of other nutrients in soils affected by ultrabasic rocks. Hence, the imbalance competition between higher amounts of available Ni and other cations in soil and root exchange complexes could result in cation leaching from the soil system, disruption of cation absorption, and interference with plant growth (Anda, 2012; Campillo-Cora et al., 2020; Jagetiya et al., 2013; Rajapaksha et al., 2012; Wang et al., 2015). Consequently, Ni distribution in peat should be monitored to achieve better plant performance and healthy agricultural productivity.

Detailed studies of Ni characteristics represented by its distribution in peat overlying an ultrabasic formation and its relationships with other peat properties are still scarce, except for some reports from laboratory-based experiments (Bartczak et al., 2018; Di Giuseppe et al., 2017; Lin et al., 2015). Therefore, the objective of this study was to reveal the characteristics of Ni in peat at several depths and several distances from the border of the ultrabasic mineral soil through its total, exchangeable, water-soluble, and adsorbed distributions. The relationships between Ni and some peat chemical properties such as pH, cation exchange capacity (CEC), and macro-and micronutrients were also examined.

## 2. Materials and methods

### 2.1 Soil Sampling

The study was conducted from March 2018 to January 2019. A straight observation line parallel to the toposequence (Fig. 1) was surveyed from the edge of peat at 121°28'53.988"E and 2°6'36.991"S toward the center of the peat at 121°28'56.717"E and 2°6'28.152"S. The study site is a backswamp between the Laa and Tambalako Rivers at Molino Village, East Petasia District, North Morowali, Central Sulawesi. Composite samples of peat material (± 1 kg) were collected using a hoe at depths of 0–30, 30–60, and 60–90 cm along the line at distances of 100, 200, 300, 400, 500, and 600 m from the border of the ultrabasic mineral soil. In total, 36 samples were collected. An additional ultrabasic mineral soil sample (± 1 kg) was taken according to the predicted source location of mineral soil.

### 2.2. Laboratory Measurements

Peat chemical analyses were carried out at the Soil Chemistry and Fertility Laboratory, Soil and Land Resources Department, Faculty of Agriculture, IPB University. Analyses of peat samples in wet conditions (similar to field conditions) included: i) measurement of water-soluble Ni using distilled water extractant equilibrated for 3 days at room temperature (25° C); ii) measurement of total Ni using a wet digestion method with $HNO_3$ and $HClO_4$ as extractants; (iii) measurement of exchangeable Ni using DTPA–TEA extractant solution consisting of 0.005 M DTPA (diethyl triamine penta-acetic acid) with 0.01 M $CaCl_2$ and 0.1 M TEA (triethanolamine) at pH 7; and (iv) determination of peat water content using the gravimetric method. The resulting solutions (soluble Ni: equilibrated Aquadest, total Ni: wet digestion, exchangeable Ni: DTPA–TEA) were measured using a Shimadzu AA-6300 atomic absorption spectrophotometer. Adsorbed Ni was calculated as the difference between the amount of exchangeable Ni and the amount of water-soluble Ni. The analysis of total Ni in ultramafic mineral soil material was conducted at the Center for Research and Development of Mineral and Coal Technology (Tekmira) Laboratory, Bandung, West Java.

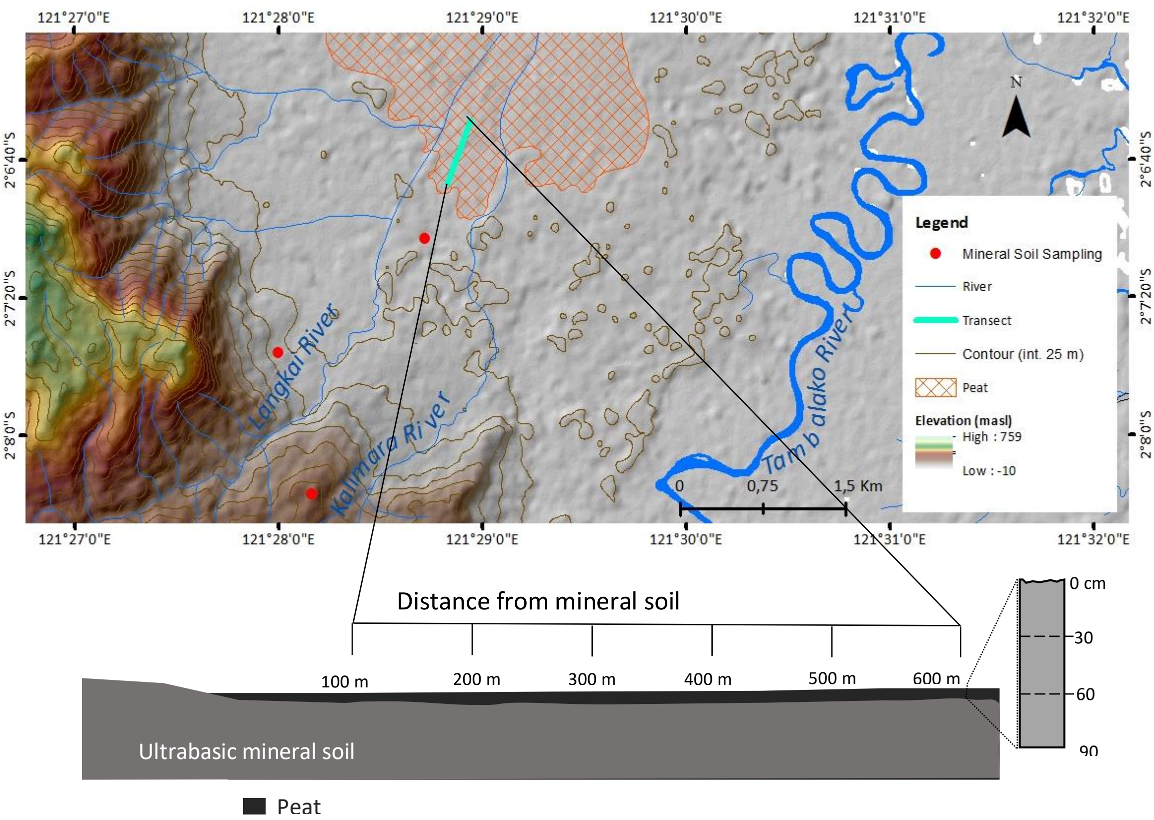


**Figure 1**. Location of study site and sampling design of this research (modified after GIA (2020) and Ritung et al. (2019)).

**Table 1**. Spearman correlation ($r_s$) between total, exchangeable, water-soluble, and adsorbed Ni with peat depth and distances from ultrabasic mineral soil

| Factors | $r_s$ (n = 36) | | | |
|---|---|---|---|---|
| | Total Ni | Exch. Ni | Water-soluble Ni | Adsorbed Ni |
| Ni Fraction | | | | |
| Total Ni | 1.00 | | | |
| Exchangeable Ni | 0.48** | 1.00 | | |
| Water-soluble Ni | 0.47** | 0.11 | 1.00 | |
| Adsorbed Ni | 0.38* | 0.96** | −0.11 | 1.00 |
| Peat Depth | −0.33* | −0.36* | 0.28 | −0.48** |
| Distances | −0.60** | −0.41* | −0.53** | −0.31 |

**Remark**: Asterisk value represents significant correlation (*p-value <0.05; ** p-value <0.01)

### 2.3. Statistical Analyses

The peat chemical data for the study site, including pH, CEC, and total and exchangeable macro- and micronutrients (K, Ca, Mg, Fe, Cu, and Zn) were provided with permission from Pulunggono et al. (2020) for comparison with Ni. Statistical processing was performed using the analysis of variance (ANOVA) method followed by Tukey's honest significance test (HSD) at a 95% confidence interval. Multiple linear regression based on peat depth, distance from ultrabasic mineral soil, and chemical data was also conducted in order to develop an equation for each Ni fraction which was plotted as a response. Macro- and micronutrient concentrations of K, Ca, Cu, and Zn were not used as predictors in multiple linear regression analyses due to their insignificant concentrations compared to Ni. The Spearman rank correlation test ($r_s$) was also carried out on the relationships between Ni and pH, CEC, water content, macro- and micronutrients, depths of peat samples, and distance from ultrabasic mineral soils based on data distribution, and supplemented with t-tests at 95% confidence intervals. Statistical analyses were performed using the computer programs Microsoft Excel and Minitab version 16.2.1.

## 3. Results

### 3.1.Total, Exchangeable, Water-Soluble, and Adsorbed Ni Distributions in Peat along the Transect

Total and exchangeable Ni in this study (Fig. 2 and Table 1) decreased significantly with increasing peat depth and distance from ultrabasic mineral soil. Adsorbed Ni correlated negatively with depth and distance. The water-soluble Ni decreased significantly with increasing distance from ultrabasic mineral soil (Table 1).

With respect to the distance from the ultrabasic mineral soil, the total and exchangeable Ni in Fig. 2 fluctuated and showed different patterns between the distances of less than 400 m and greater than 400 meters. At distances of less than 400 meters from the ultrabasic mineral soil, exchangeable Ni tended to decrease, ranging from around 40 to 60% of total Ni. Meanwhile, total Ni tended to increase with distance. By contrast, exchangeable Ni tended to increase at distances of 500 to 600 meters, ranging from about 70 to 90% of total Ni, while total Ni tended to decrease with increasing distance. Moreover, the exchangeable Ni extracted by DTPA consisted mainly of the adsorbed fraction (around 77 to 99%) and a small amount of water-soluble Ni (about 1 to 23%).

The Ni in peat at the study site inherited from ultrabasic mineral soil is shown in Table 1. A higher nickel content was also recorded by Fu et al. (2014) at the same geological formation. Ni recorded in this study had a higher standard deviation, possibly due to different sources of ultrabasic mineral soil sampling.

### 3.2. Relationships Between Ni and Several Chemical Soil Properties

The total and exchangeable macro- and micronutrients are modified after Pulunggono et al. (2020), and shown in Fig. 3 and Fig. 4. The amounts of total and exchangeable Mg were highest, compared to K and Ca. In comparison with Ni (Fig. 3), the total and exchangeable Mg showed equivalent contents (avg. 116.08% and 91.44%, respectively). However, very low contents of K and Ca were recorded in this study, which indicates the leaching process. With respect to the distance from the mineral soil, the macronutrient K showed a pattern similar to that of Ni, while Ca and Mg showed no clear patterns. The total and exchangeable K contents were relatively higher at distances of less than 400 meters than at greater distances. By contrast, total and exchangeable Ca and Mg fluctuated and were not affected by increasing distance. Total K, Ca, and Mg tended to decrease with depth.

According to Fig. 4 and Pulunggono et al. (2020), the total and exchangeable contents of micronutrients in peat at the study site were lower compared to the Ni concentration. The total contents of all the micronutrients decreased with increasing depth, showing a similar distribution pattern to total Ni (Fig. 2). Therefore, the total distribution of micronutrients in peat at all distances from ultrabasic mineral soil showed a contrasting pattern compared to their exchangeable forms. The total Cu and Zn showed correlations with distance from ultrabasic mineral soil identical to that of total Ni; however, total Fe fluctuated and tended to correlate negatively with distance. In contrast to exchangeable Ni, the concentration of exchangeable Fe, Cu, and Zn increased significantly with increasing distance from the ultrabasic mineral soil (Fig. 2, Fig. 4; Pulunggono et al. (2020).

Cation exchange capacity and peat water content in Fig. 5 increased with increasing distance from ultrabasic mineral soil; however, only the latter showed a notable relationship

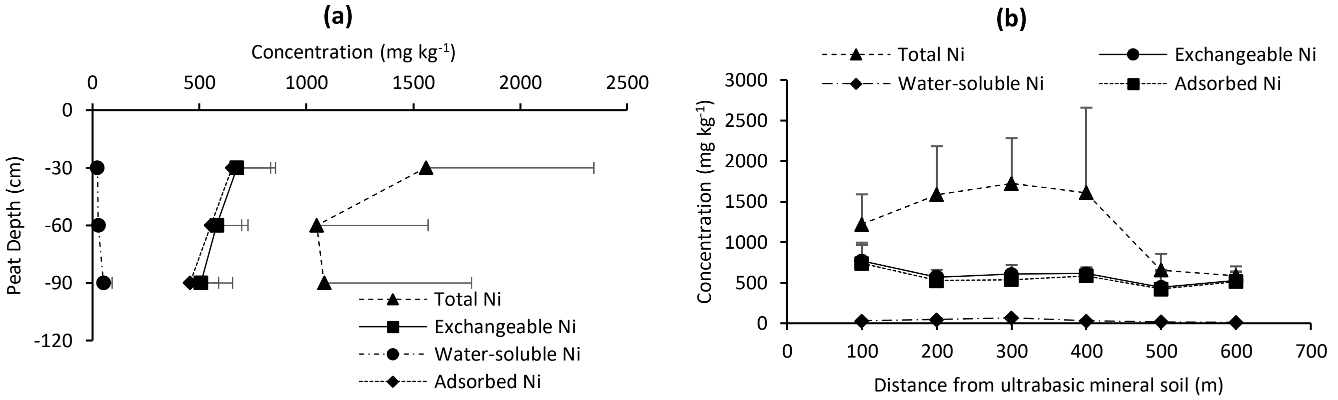


**Figure 2.** Total, exchangeable, water-soluble, and adsorbed Ni distribution in peat: **(a)** based on peat depth, and **(b)** based on distance from ultrabasic mineral soil.

($r_s$ = 0.19, $p > 0.05$; 0.54, $p < 0.05$; respectively). Meanwhile, all of these parameters showed a significant positive correlation with depth (Fig. 5; Pulunggono et al. (2020).

In general, macronutrients showed an irregular pattern in their relationship with all observed Ni fractions compared to micronutrients (Table 3). Total and exchangeable K contents, which were reported to be relatively lower than the others, presented significant positive correlations with total and water-soluble Ni, whereas Mg, recognized as the nutrient with the highest concentrations, only showed a significant relationship with water-soluble Ni. On the other hand, despite several small values, both total and exchangeable micronutrient fractions showed a relatively uniform relationship with whole observed Ni fractions. All exchangeable micronutrients correlated negatively with the whole Ni fractions, particularly for exchangeable Fe, which had significant relationships with total, exchangeable, and water-soluble Ni. Meanwhile, the opposite relationship was observed for their total contents. The total Fe, Cu, and Zn correlated significantly with total Ni. Furthermore, total Cu also had a significant positive correlation with exchangeable and adsorbed Ni.

The multiple linear regression analysis (Fig. 6) showed that the peat depth, pH, and distance from ultrabasic mineral soil exhibited a remarkable influence on exchangeable and adsorbed Ni. Furthermore, the same analysis also showed the notable importance of exchangeable Fe in governing total Ni content in peat at the study site. The water-soluble Ni was strongly controlled by depth. The relationships between all observed parameters and each Ni fraction are presented in Equations 1–4.

$$\text{Total Ni} = 891 - 0.630\ \text{Distance} - 3.45\ \text{Depth} + 0.356\ \text{Exch Mg} - 3.81\ \text{Exch Fe} + 0.580\ \text{Total Mg} + 1.17\ \text{Total Fe} + 1.88\ \text{CEC} - 41\ \text{pH} + 0.60\ \text{Water Content} \quad \text{[Eq. 1]}$$

$$\text{Exchangeable Ni} = 2074 - 0.639\ \text{Distance} - 7.36\ \text{Depth} - 0.0114\ \text{Total Ni} + 0.0013\ \text{Exch Mg} - 0.122\ \text{Exch Fe} - 0.0238\ \text{Total Mg} - 0.070\ \text{Total Fe} + 0.36\ \text{CEC} - 216.0\ \text{pH} + 0.267\ \text{Water Content} \quad \text{[Eq. 2]}$$

$$\text{Water Soluble Ni} = -7.2 + 0.00844\ \text{Total Ni} + 0.0112\ \text{Distance} + 0.720\ \text{Depth} + 0.0089\ \text{Exch Mg} - 0.0712\ \text{Exch Fe} - 0.0040\ \text{Total Mg} + 0.0599\ \text{Total Fe} + 0.367\ \text{CEC} - 2.1\ \text{pH} - 0.0907\ \text{Water Content} \quad \text{[Eq. 3]}$$

$$\text{Adsorbed Ni} = 2081 - 0.0199\ \text{Total Ni} - 0.651\ \text{Distance} - 8.08\ \text{Depth} - 0.0077\ \text{Exch Mg} - 0.051\ \text{Exch Fe} - 0.0198\ \text{Total Mg} - 0.130\ \text{Total Fe} - 0.00\ \text{CEC} - 213.9\ \text{pH} + 0.358\ \text{Water Content} \quad \text{[Eq. 4]}$$

## 4. Discussion

The high Ni content in the peat did not originate from organic parent material; rather, it derived from ultrabasic mineral soil with high Ni content. According to Takada et al. (2016) and Hodgkins et al. (2018), tropical peatland developed from ferns, woody angiosperms, and gymnosperm vegetation. Trace elements are released in very low quantities from decomposition of the organic material (Armanto, 2019; Hosokawa et al., 2016; Nelvia, 2018; Sutejo et al., 2017). Topography analysis through field observation and the National Digital Elevation Model (GIA (2020); Fig. 1) showed that the study area is situated in a valley that accommodated the downstream flow of permanent and intermittent streams, which transported material high in Ni content from the upslope area (Table 1). Fu et al. (2014) reported that soil at the study site overlies Ni-rich ultrabasic rocks consisting mainly of lherzolite, harzburgite, and peridotite.

**Table 2.** Total Fe and Ni from ultrabasic mineral soil adjacent to the toposequence

| Element | Total (mg $kg^{-1}$) | | | Information and reference |
|---|---|---|---|---|
| Nickel (Ni) | 4,367 | ± | 2,155 | Mineral soil, study site |
| Iron (Fe)<br>Zinc (Zn)<br>Copper (Cu) | 249,300<br>257<br>110 | ±<br>±<br>± | 101,183<br>65<br>17 | Mineral soil, study site, Pulunggono et al. (2020) |
| Iron (Fe)<br>Nickel (Ni) | 62,319.79<br>2,043.08 | | | Ultrabasic bedrock, Fu et al. (2014) |

**Table 3**. Spearman correlation ($r_s$) between total, exchangeable, water-soluble, and adsorbed Ni with peat chemical properties

| Factors | $r_s$ (n = 36) | | | |
|---|---|---|---|---|
| | Total Ni | Exch. Ni | Water-soluble Ni | Adsorbed Ni |
| Macronutrients | | | | |
| Exch. K | 0.64** | 0.15 | 0.58** | 0.04 |
| Exch. Ca | 0.37* | 0.16 | 0.32 | 0.15 |
| Exch. Mg | 0.31 | 0.05 | 0.38* | −0.02 |
| Total K | 0.66** | 0.19 | 0.45** | 0.15 |
| Total Ca | 0.08 | −0.01 | −0.16 | 0.03 |
| Total Mg | 0.29 | 0.03 | 0.02 | 0.05 |
| Micronutrients | | | | |
| Exch. Fe | −0.77** | −0.42* | −0.38* | −0.32 |
| Exch. Cu | −0.31 | −0.23 | −0.42* | −0.20 |
| Exch. Zn | −0.31 | −0.19 | −0.16 | −0.24 |
| Total Fe | 0.51** | 0.23 | 0.01 | 0.27 |
| Total Cu | 0.61** | 0.56** | 0.22 | 0.48** |
| Total Zn | 0.78** | 0.37* | 0.42* | 0.28 |
| Other peat properties | | | | |
| pH $H_2O$ | −0.17 | −0.00 | −0.12 | 0.09 |
| CEC | −0.35* | −0.01 | −0.13 | 0.01 |
| Water content | −0.46** | −0.23 | −0.27 | −0.20 |

Remark: Asterisk value represents significant correlation (*p-value <0.05; ** p-value <0.01)

The distribution of Ni in peat is determined by the degree and contribution of the heterogeneous soil fraction at the peat edge, which tends to become homogenous towards the center of the peat. Close to the border, the peat has a thin organic layer and some amounts of mineral soil containing Ni that originated from an elevated area and from below in the substratum, mixed with different decomposition stages of organic material. In this area, Ni movement and distribution are regulated by organic acids (Antić-Mladenović et al., 2017; Rinklebe et al., 2016) combined with pH (Ma et al., 2013), water content (Bartczak et al., 2018), and the presence of ultrabasic-derived soil materials such as clay (Osakwe, 2013; van der Ent et al., 2016), Fe oxides and Fe oxy-hydroxides (Antić-Mladenović et al., 2017; Bani et al., 2014; Rinklebe et al., 2016).

Based on multiple regression and Spearman rank correlation analyses, our results seem consistent with the statement above and indicate that Ni distributions in peat at the study transect were correlated significantly with a combination of Fe, pH, organic material (presenting as CEC and adsorbed Ni), and water content, with significant effects due to peat depth and distance from ultrabasic mineral soil (Fig. 6, Table 2, and Table 3). The depth was recorded as the strongest factor controlling exchangeable, water-soluble, and adsorbed Ni distributions (Fig. 6). The concentrations of these fractions are also dictated by the total Ni (Table 2). Peat alongside the transect was classified as thick peat (200–300 cm) in the hemic decomposition stage (Ritung et al., 2019), indicating that the peat organic material had been moderately decomposed, which contributes high CEC. The peat might be contaminated with mineral soil, as discussed below (Pulunggono et al. (2020); Fig. 5).

According to previous evidence, soil acidity influences the dissolution and precipitation of Ni in soil solutions (Antić-Mladenović et al., 2017; de Macedo et al., 2016; Ma et al., 2013). Our results, however, showed no significant correlation of soil acidity or pH with Ni fractions (Table 3). No significant relationship was found between pH and any observed Ni soluble fraction in Table 3, indicating that pH was not the factor defining Ni distribution in peat at the study site, which was also described well by the multiple regression in Fig. 6. Similar results were also reported by (D'Amico & Previtali, 2012) in ultrabasic derived mineral soil

Exchangeable Ni (Fig. 2) was dominated by adsorbed Ni with a small amount of water-soluble Ni. CEC was the second most important factor controlling water-soluble Ni, which is the most labile part of Ni (Fig. 6). However, the high CEC in Fig. 5 indicated that the soil exchange complex was composed mainly of organic substances. This indicates that most Ni in peat at the study site was bonded to the soil organic exchange complex, which could be exchanged by DTPA. Other research also found similar results (Koistinen et al., 2015).

Similar to other findings (Antić-Mladenović et al., 2017; Antić-Mladenović et al., 2011; Rinklebe & Shaheen, 2014), Fe in this study exhibited a strong relationship with Ni, marked by significant influence in the multiple regression analysis (Fig. 6) and strong negative correlations of its exchangeable fraction with total, exchangeable, and water-soluble Ni (Table 3). The total Fe also showed a significant positive correlation with total Ni. The significant correlation of Fe with Ni would reflect the reduction of peat water content due to the establishment of drainage canals for oil palm plantations. This causes the formation of Fe oxides or Fe oxy-hydroxides under aerobic conditions and low water contents (Cabala et al., 2013).

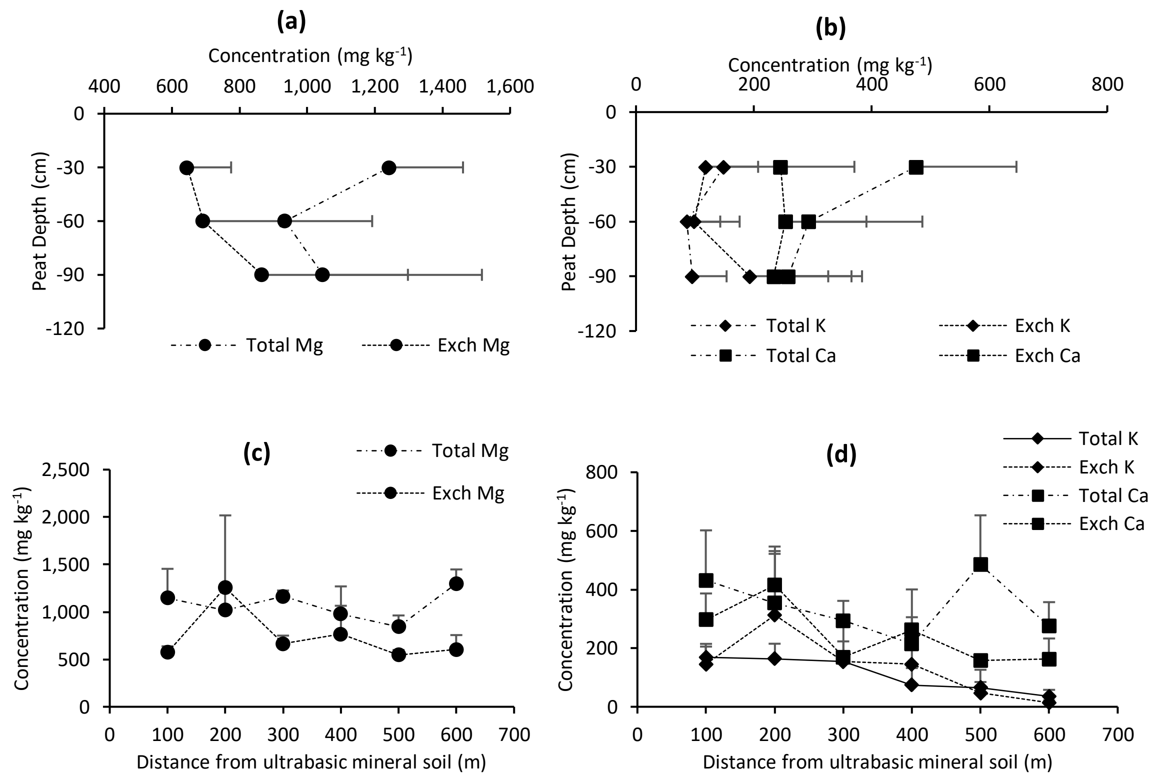


Figure 3. Total and exchangeable macronutrients of K, Ca, and Mg in peat. **(a)** Total and exchangeable Mg based on depth, **(b)** total and exchangeable K and Ca based on depth, **(c)** total and exchangeable Mg based on distance from ultrabasic mineral soil, and **(d)** total and exchangeable K and Ca based on distance from ultrabasic mineral soil (reprinted by permission from Pulunggono et al. (2020)).

Even though Fe in the form of $Fe^{2+}$ may compete with Ni in root and soil exchange complexes (Melo et al., 2014; Yusuf et al., 2011), Ni has a high affinity for and bonds to Fe oxides in high pH (Alves et al., 2011; Sheng et al., 2018; Sipos et al., 2014). Furthermore, other researchers have reported that Ni may be co-precipitated with $Fe(OH)_3$ during $Fe^{2+}$ oxidation (Antić-Mladenović et al., 2017; Bani et al., 2014; Frohne et al., 2014). This process, on our study site, occurs at the peat surface, which has a relatively high pH and contains high Fe. Cu and Zn also showed a tendency to compete with Ni in exchange complexes (Table 3; Aziz et al. (2015); Melo et al. (2014); Nishida et al. (2015); Sabir et al. (2014)), although both cations had insignificant concentrations compared to Ni (Fig. 4).

The values and standard deviations of total Ni increased with distance from 100 to 400 meters from ultrabasic mineral soil. However, total Ni fell below 900 mg $kg^{-1}$ with low standard deviation at distances of 500 and 600 meters. Moreover, Fig. 4 shows that exchangeable Fe at distances of less than 400 meters ranged from about 1.5 to 2 times higher than that found at greater distances, with a similar pattern found for exchangeable Ni. Furthermore, CEC in Fig. 5 tended to increase with increasing peat depth and distance from ultrabasic mineral soil. These results indicate the accumulation of the mineral soil fraction, the formation of Fe oxides/oxy-hydroxides, and/or co-precipitation of Ni–Fe in the peat surface at distances of less than 400 meters from mineral soil. Exchangeable Ni decreased due to fixation by Fe oxides and eventually failed to be chelated by DTPA extraction, as represented by the wide gap between exchangeable and total Ni contents at this distance (Fig. 2). Furthermore, organic acids may play a primary role in Ni dissolution and exchangeability at farther distances according to the increasing soil acidity and CEC (Fig. 5) and also the 100 % Fe dissolution (Fig. 4).

The water-soluble Ni in peat (Fig. 2) tended to increase with increasing depth, while the adsorbed Ni decreased significantly. These results indicate the difference in organic material decomposition level between the peat surface and the deeper layer. Compared to the deeper layer, the organic material at the peat surface is more exposed to the decomposition process and frequent drying due to the movement of the groundwater table (Nurzakiah et al., 2014; Nurzakiah et al., 2020); these enhance aerobic oxidation (Wakhid et al., 2017) and increase CEC (Armanto, 2019). Hence, Ni is adsorbed more on the organic matter at the surface that has a higher capacity of organic exchange sites than in the deeper layer that relatively remains intact. However, the CEC values obtained in this study (Fig. 5) showed the opposite pattern. These results may have occurred due to the movement of mineral soil covering the peat surface.

In general, Ni had a positive charge, similar to H and the macronutrients of K, Ca, and Mg. This can lead to competition among these cations in the soil and on root cation exchange sites. However, the exchangeable K, Ca, and Mg did not correlate with Ni as shown in Table 3. It seems that the amount of Ni on the soil exchange sites is not affected by its competition with K, Ca, and Mg. At the study site, exchangeable and total K and Ca were relatively low compared to exchangeable and total Ni (Fig. 2, Fig. 3).

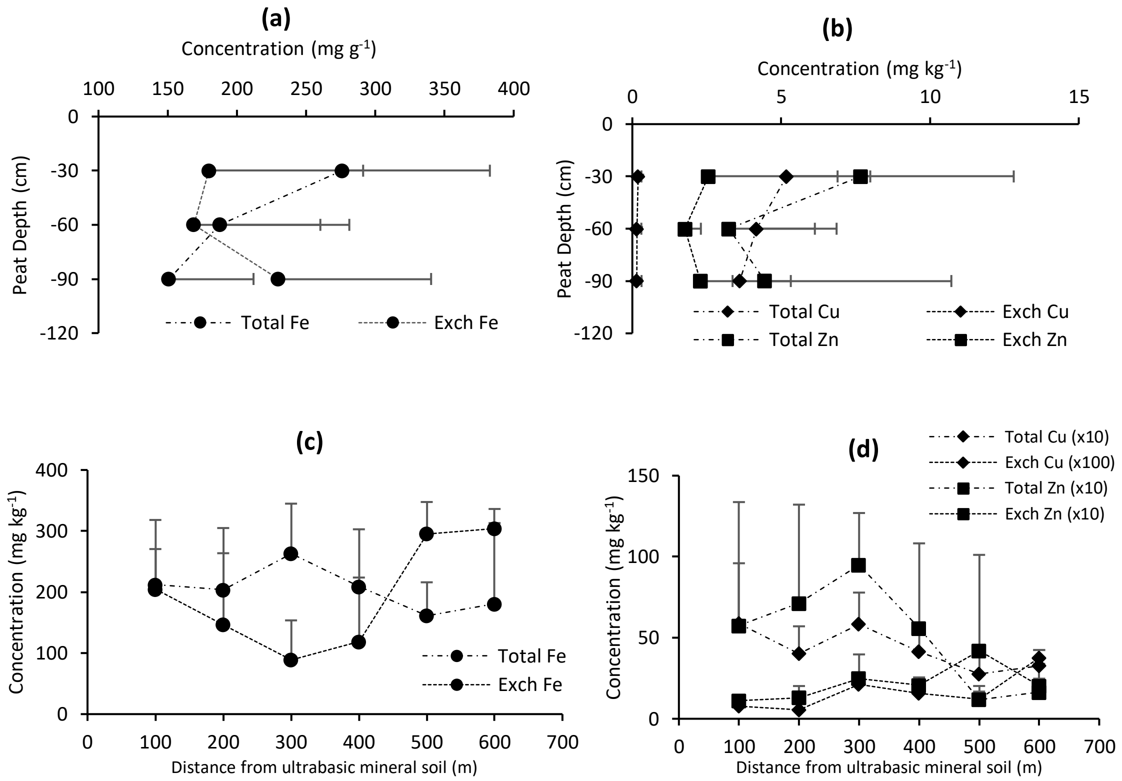


Figure 4. Total and exchangeable micronutrients of Fe, Cu, and Zn in peat. **(a)** Total and exchangeable Fe based on depth, **(b)** total and exchangeable Cu and Zn based on depth, **(c)** total and exchangeable Fe based on distance from ultrabasic mineral soil, and **(d)** total and exchangeable Cu and Zn based on distance from ultrabasic mineral soil (reprinted by permission from Pulunggono et al. (2020)).

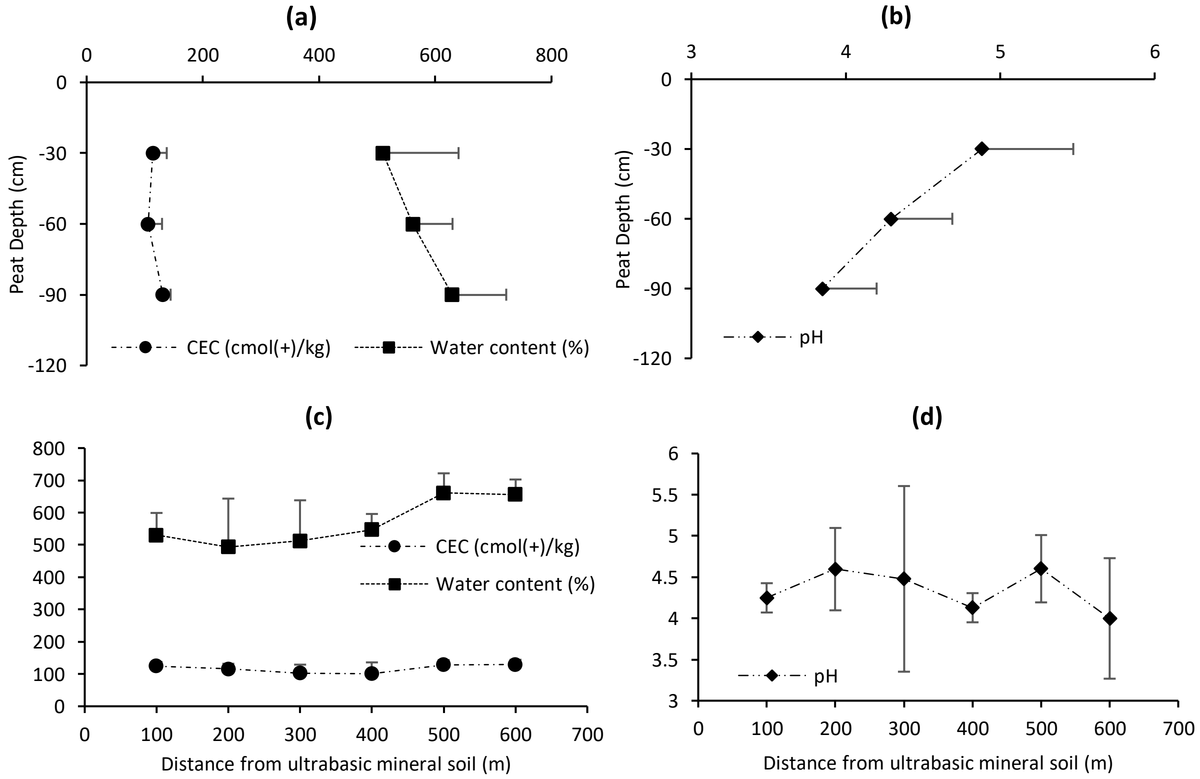


Figure 5. Peat soil properties at the study site. **(a)** CEC and water content based on depth, **(b)** pH based on depth, **(c)** CEC and water content based on distance from ultrabasic mineral soil, and **(d)** pH based on distance from ultrabasic mineral soil (reprinted by permission from Pulunggono et al. (2020)).

Melo et al. (2014) showed that Ni showed less affinity with peat compared to Cu, Fe, and Co, whereas the organic-Ni complexes were more stable than those of Mn and Zn. Consistent with this study, weak relationships between Ni and K and Ca in plant roots and on soil exchange complexes are also reported by other researchers (Aziz et al., 2015; Lin et al., 2015). Meanwhile, exchangeable and total Mg showed similar contents compared to exchangeable and total Ni (avg. 91% and 116 %, respectively). Mg (Table 3), relying on mass action, may inhibit Ni absorption by plant roots. According to Jiang et al. (2017) and Amjad et al. (2020), Mg had an antagonistic effect on Ni in the root zone. High total Ni would not cause hazardous effects for human and animal health due to its low availability at the near-neutral pH of mineral soil (Banerjee & Roychoudhury, 2020; Gonnelli & Renella, 2013). However, low pH was detected in peat soil at the study site (Fig. 5). This can increase available Ni that can be absorbed by the plant roots and enter the food chain (Olafisoye et al., 2020; Sreekanth et al., 2013; Zhang et al., 2015). The water-soluble Ni in soil solution (Fig. 2) is also identified at levels higher than the 0.1–0.5 mg $kg^{-1}$ defined as a critical level for plant phytotoxicity (Gonnelli & Renella, 2013).

The domination of Ni in soil solution and exchange complexes enhances plant root preference in absorbing and accumulating Ni in its tissues (Hassan et al., 2019; Sreekanth et al., 2013; Wang et al., 2015). An elevated Ni concentration in plant tissue inhibits root development (Abd_Allah et al., 2019; Uruç Parlak, 2016), stimulates electrolyte leakage (Yusuf et al., 2012), and disrupts the photosynthesis process (Awasthi & Sinha, 2013; Khair et al., 2020; Mahmood et al., 2016). Unfortunately, there is no reported data for the assessment of Ni in palm oil and its derivatives that originated in this area.

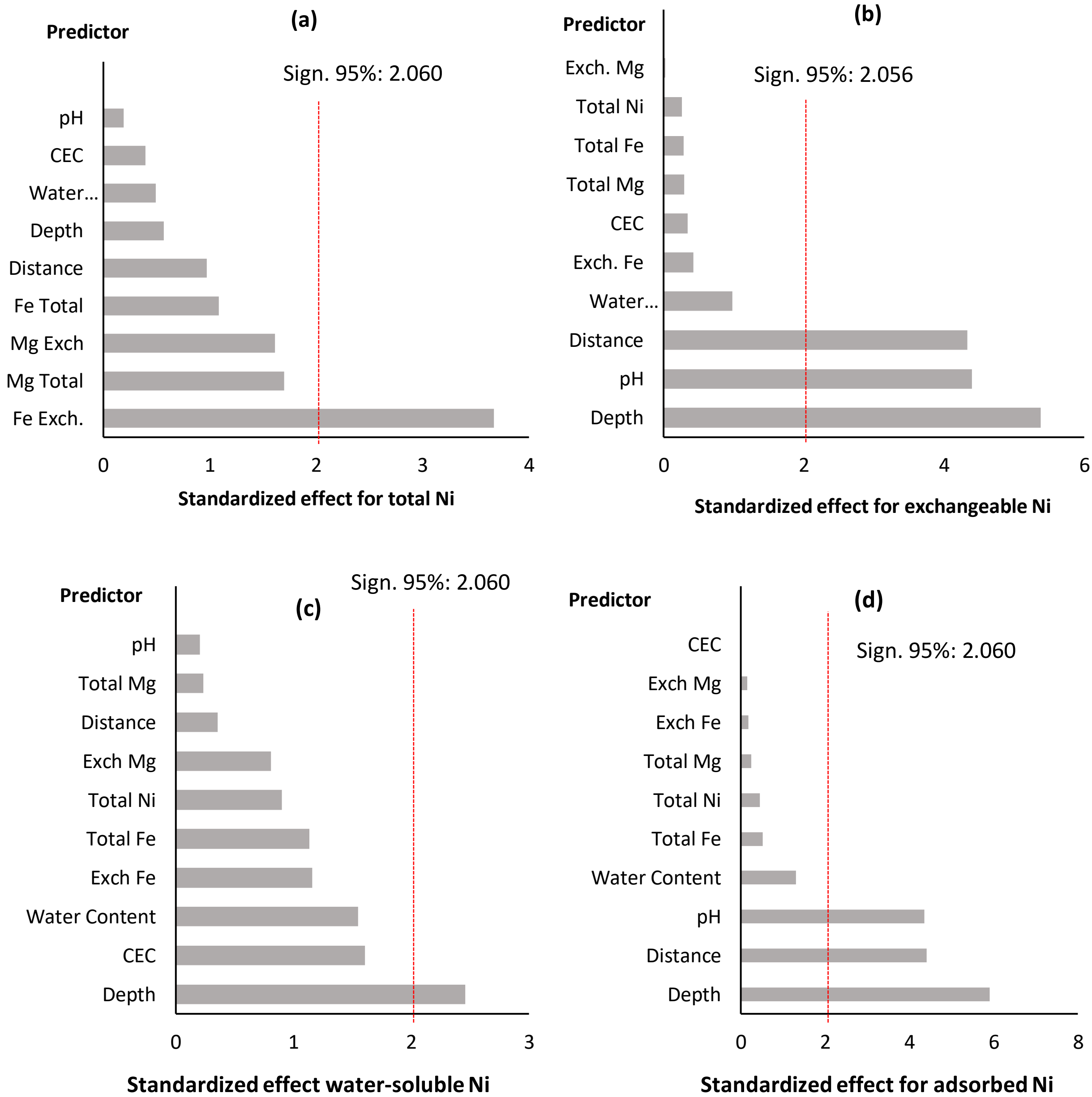


Figure 6. Multiple regression standardized effects plots for total Ni **(a)**, exchangeable Ni **(b)**, water-soluble Ni **(c)**, and adsorbed Ni as a response **(d)** (Remarks: Predictors/factors that exceeded the dotted line are considered significant)

## 5. Conclusion

The high Ni content in peat at the study transect is caused by Ni accumulation in a valley that accommodated the downstream flow of permanent and intermittent river streams, which transported material high in Ni content from the hilly area. Ni distribution in peat at the study transect is mainly governed by the combination of Fe, organic material (presenting as CEC and adsorbed Ni), and water content, reflecting significant effects of peat depth and distance from ultrabasic mineral soil. The depth was recorded as the strongest significant factor that controlled exchangeable, water-soluble, and adsorbed Ni distribution. There is an indication of mineral soil fraction accumulation in the peat surface at distances of 100–400 meters from the ultrabasic mineral soil, as indicated by the values, standard deviations, and patterns of Ni, CEC, and Fe contents.

## Acknowledgements

The authors gratefully thank Prof. Dr. Ir. Supiandi Sabiham M.Agr., Dr. Ir. Arief Hartono M.Sc., and Siti Nurzakiah M.S for the critical comments and constructive suggestions that substantially improved the depth and clarity of the manuscript. We also thank Lina Lathifah Nurazizah, B.Agr. for her help in handling the laboratory analysis.

## Declaration of Competing Interest

The authors declare no competing financial or personal interests that may appear and influence the work reported in this paper.

## References

Abat, M., McLaughlin, M. J., Kirby, J. K., & Stacey, S. P. (2012). Adsorption and desorption of copper and zinc in tropical peat soils of Sarawak, Malaysia. *Geoderma*, *175-176*, 58-63. https://doi.org/10.1016/j.geoderma.2012.01.024

Abd_Allah, E. F., Hashem, A., Alam, P., & Ahmad, P. (2019). Silicon Alleviates Nickel-Induced Oxidative Stress by Regulating Antioxidant Defense and Glyoxalase Systems in Mustard Plants. *Journal of Plant Growth Regulation*, *38*(4), 1260-1273. https://doi.org/10.1007/s00344-019-09931-y

Alves, S., Trancoso, M. A., Gonçalves, M. d. L. S., & Correia dos Santos, M. M. (2011). A nickel availability study in serpentinised areas of Portugal. *Geoderma*, *164*(3), 155-163. https://doi.org/10.1016/j.geoderma.2011.05.019

Amjad, M., Raza, H., Murtaza, B., Abbas, G., Imran, M., Shahid, M., Naeem, M. A., Zakir, A., & Iqbal, M. M. (2020). Nickel Toxicity Induced Changes in Nutrient Dynamics and Antioxidant Profiling in Two Maize (*Zea mays* L.) Hybrids. *Plants*, *9*(1), 5. https://doi.org/10.3390/plants9010005

Anda, M. (2012). Cation imbalance and heavy metal content of seven Indonesian soils as affected by elemental compositions of parent rocks. *Geoderma*, *189-190*, 388-396. https://doi.org/10.1016/j.geoderma.2012.05.009

Antić-Mladenović, S., Frohne, T., Kresović, M., Stärk, H.-J., Tomić, Z., Ličina, V., & Rinklebe, J. (2017). Biogeochemistry of Ni and Pb in a periodically flooded arable soil: Fractionation and redox-induced (im)mobilization. *Journal of Environmental Management*, *186*, 141-150. https://doi.org/10.1016/j.jenvman.2016.06.005

Antić-Mladenović, S., Rinklebe, J., Frohne, T., Stärk, H.-J., Wennrich, R., Tomić, Z., & Ličina, V. (2011). Impact of controlled redox conditions on nickel in a serpentine soil. *Journal of Soils and Sediments*, *11*(3), 406-415. https://doi.org/10.1007/s11368-010-0325-0

Armanto, M. E. (2019). Comparison of Chemical Properties of Peats under Different Land Uses in South Sumatra, Indonesia [journal article]. *Journal of Ecological Engineering*, *20*(5), 184-192. https://doi.org/10.12911/22998993/105440

Awasthi, K., & Sinha, P. (2013). Nickel stress induced antioxidant defence system in sponge gourd (*Luffa cylindrical*). *Journal of Plant Physiology & Pathology*, *1*(1), 5. https://doi.org/10.4172/2329-955X.1000102

Aziz, H., Sabir, M., Ahmad, H. R., Aziz, T., Zia - ur - Rehman, M., Hakeem, K. R., & Ozturk, M. (2015). Alleviating effect of calcium on nickel toxicity in rice. *Clean–Soil, Air, Water*, *43*(6), 901-909. https://doi.org/10.1002/clen.201400085

Banerjee, A., & Roychoudhury, A. (2020). Plant Responses to Environmental Nickel Toxicity. In *Plant Micronutrients* (pp. 101-111). Springer. https://doi.org/10.1007/978-3-030-49856-6

Bani, A., Echevarria, G., Montargès-Pelletier, E., Gjoka, F., Sulçe, S., & Morel, J. L. (2014). Pedogenesis and nickel biogeochemistry in a typical Albanian ultramafic toposequence. *Environmental Monitoring and Assessment*, *186*(7), 4431-4442. https://doi.org/10.1007/s10661-014-3709-6

Bartczak, P., Norman, M., Klapiszewski, Ł., Karwańska, N., Kawalec, M., Baczyńska, M., Wysokowski, M., Zdarta, J., Ciesielczyk, F., & Jesionowski, T. (2018). Removal of nickel(II) and lead(II) ions from aqueous solution using peat as a low-cost adsorbent: A kinetic and equilibrium study. *Arabian Journal of Chemistry*, *11*(8), 1209-1222. https://doi.org/10.1016/j.arabjc.2015.07.018

Cabala, J., Smieja-Król, B., Jablonska, M., & Chrost, L. (2013). Mineral components in a peat deposit: looking for signs of early mining and smelting activities in Silesia–Cracow region (Southern Poland). *Environmental Earth Sciences*, *69*(8), 2559-2568. https://doi.org/10.1007/s12665-012-2080-6

Campillo-Cora, C., Conde-Cid, M., Arias-Estévez, M., Fernández-Calviño, D., & Alonso-Vega, F. (2020). Specific Adsorption of Heavy Metals in Soils: Individual and Competitive Experiments. *Agronomy*, *10*(8), 1113. https://www.mdpi.com/2073-4395/10/8/1113

D'Amico, M. E., & Previtali, F. (2012). Edaphic influences of ophiolitic substrates on vegetation in the Western Italian Alps. *Plant and Soil*, *351*(1), 73-95. https://doi.org/10.1007/s11104-011-0932-6

Das, K. K., Reddy, R. C., Bagoji, I. B., Das, S., Bagali, S., Mullur, L., Khodnapur, J. P., & Biradar, M. S. (2019). Primary concept of nickel toxicity – an overview. *Journal of Basic and Clinical Physiology and Pharmacology*, *30*(2), 141-152. https://doi.org/doi:10.1515/jbcpp-2017-0171

de Macedo, F. G., Bresolin, J. D., Santos, E. F., Furlan, F., Lopes da Silva, W. T., Polacco, J. C., & Lavres, J. (2016). Nickel Availability in Soil as Influenced by Liming and Its Role in Soybean Nitrogen Metabolism [Original Research]. *Frontiers in Plant Science*, *7*(1358). https://doi.org/10.3389/fpls.2016.01358

Di Giuseppe, D., Melchiorre, M., Faccini, B., Ferretti, G., & Coltorti, M. (2017). Effects of middle-term land reclamation on nickel soil-water interaction: a case study from reclaimed salt marshes of Po River Delta, Italy. *Environmental Monitoring and Assessment*, *189*(10), 523. https://doi.org/10.1007/s10661-017-6240-8

Frohne, T., Rinklebe, J., & Diaz-Bone, R. A. (2014). Contamination of Floodplain Soils along the Wupper River, Germany, with As, Co, Cu, Ni, Sb, and Zn and the Impact of Pre-definite Redox Variations on the Mobility of These Elements. *Soil and Sediment Contamination: An International Journal*, *23*(7), 779-799. https://doi.org/10.1080/15320383.2014.872597

Fu, W., Yang, J., Yang, M., Pang, B., Liu, X., Niu, H., & Huang, X. (2014). Mineralogical and geochemical characteristics of a serpentinite-derived laterite profile from East Sulawesi, Indonesia: Implications for the lateritization process and Ni supergene enrichment in the tropical rainforest. *Journal of Asian Earth Sciences*, *93*, 74-88. https://doi.org/10.1016/j.jseaes.2014.06.030

Genchi, G., Carocci, A., Lauria, G., Sinicropi, M. S., & Catalano, A. (2020). Nickel: Human Health and Environmental Toxicology. *International Journal of Environmental Research and Public Health*, *17*(3), 679. https://www.mdpi.com/1660-4601/17/3/679

GIA, G. I. A. B. B. I. G. (2020). *National Digital Elevation Model. Tiles: 2213-433_v1.0; 2213-431_v1.0; 2113-644_v1.0; and 2113-642_v1.0*. Badan Informasi Geospasial. Cibinong (ID). http://tides.big.go.id/DEMNAS/DEMNAS.php

Gonnelli, C., & Renella, G. (2013). Chromium and nickel. In B. Alloway (Ed.), *Heavy Metals in Soils. Environmental Pollution* (Vol. 22, pp. 313-333). Springer, Dordrecht. https://doi.org/10.1007/978-94-007-4470-7_11

Hassan, M. U., Chattha, M. U., Khan, I., Chattha, M. B., Aamer, M., Nawaz, M., Ali, A., Khan, M. A. U., & Khan, T. A. (2019). Nickel toxicity in plants: reasons, toxic effects, tolerance mechanisms, and remediation possibilities—a review. *Environmental Science and Pollution Research*, *26*(13), 12673-12688. https://doi.org/10.1007/s11356-019-04892-x

Hodgkins, S. B., Richardson, C. J., Dommain, R., Wang, H., Glaser, P. H., Verbeke, B., Winkler, B. R., Cobb, A. R., Rich, V. I., Missilmani, M., Flanagan, N., Ho, M., Hoyt, A. M., Harvey, C. F., Vining, S. R., Hough, M. A., Moore, T. R., Richard, P. J. H., De La Cruz, F. B., Toufaily, J., Hamdan, R., Cooper, W. T., & Chanton, J. P. (2018). Tropical peatland carbon storage linked to global latitudinal trends in peat recalcitrance. *Nature Communications*, *9*(1), 3640. https://doi.org/10.1038/s41467-018-06050-2

Hosokawa, S., Konuma, S., & Nakamura, Y. (2016). Accumulation of Trace Metal Elements (Cu, Zn, Cd, and Pb) in Surface Sediment via Decomposed Seagrass Leaves: A Mesocosm Experiment Using *Zostera marina* L. *PLoS One*, *11*(6), e0157983. https://doi.org/10.1371/journal.pone.0157983

Jagetiya, B., Soni, A., & Yadav, S. (2013). Effect of nickel on plant water relations and growth in green gram. *Indian Journal of Plant Physiology*, *18*(4), 372-376. https://doi.org/10.1007/s40502-013-0053-8

Jiang, X., Zou, B., Feng, H., Tang, J., Tu, Y., & Zhao, X. (2019). Spatial distribution mapping of Hg contamination in subclass agricultural soils using GIS enhanced multiple linear regression. *Journal of Geochemical Exploration*, *196*, 1-7. https://doi.org/10.1016/j.gexplo.2018.10.002

Jiang, Y., Gu, X., Zhu, B., & Gu, C. (2017). Development and validation of abiotic ligand model for nickel toxicity to wheat (*Triticum aestivum*). *Journal of Environmental Sciences*, *62*, 22-30. https://doi.org/10.1016/j.jes.2017.06.005

Khair, K. U., Farid, M., Ashraf, U., Zubair, M., Rizwan, M., Farid, S., Ishaq, H. K., Iftikhar, U., & Ali, S. (2020). Citric acid enhanced phytoextraction of nickel (Ni) and alleviate *Mentha piperita* (L.) from Ni-induced physiological and biochemical damages. *Environmental Science and Pollution Research*, *27*(21), 27010-27022. https://doi.org/10.1007/s11356-020-08978-9

Koistinen, M. P., Kujala, K., & Rönkkömäki, H. (2015). Adsorption of Ni(II) and Cd(II) in Compacted Peat and the Utilization of the Adsorption Properties in Hydraulic-Barrier Layers in Tailing Impoundments. *Journal of Environmental Engineering*, *141*(5), 04014086. https://doi.org/10.1061/(ASCE)EE.1943-7870.0000916

Lin, Y., Di Toro, D. M., & Allen, H. E. (2015). Development and validation of a terrestrial biotic ligand model for Ni toxicity to barley root elongation for non-calcareous soils. *Environmental Pollution*, *202*, 41-49. https://doi.org/10.1016/j.envpol.2015.03.015

Ma, Y., Lombi, E., McLaughlin, M. J., Oliver, I. W., Nolan, A. L., Oorts, K., & Smolders, E. (2013). Aging of nickel added to soils as predicted by soil pH and time. *Chemosphere*, *92*(8), 962-968. https://doi.org/10.1016/j.chemosphere.2013.03.013

Mahmood, S., Ishtiaq, S., Yasin, G., & Irshad, A. (2016). Dose dependent rhizospheric Ni toxicity evaluation: Membrane stability and antioxidant potential of Vigna species. *Chilean journal of agricultural research*, *76*, 378-384. http://www.scielo.cl/scielo.php?script=sci_arttext&pid=S0718-58392016000300017&nrm=iso

Melo, C. d. A., Oliveira, L. K. d., Goveia, D., Fraceto, L. F., & Rosa, A. H. (2014). Enrichment of tropical peat with micronutrients for agricultural applications: evaluation of adsorption and desorption processes. *Journal of the Brazilian Chemical Society*, *25*(1), 36-49. https://doi.org/10.5935/0103-5053.20130265

Nelvia, N. (2018). The Use of Fly Ash in Peat Soil on the Growth and Yield of Rice. *AGRIVITA, Journal of Agricultural Science*, *40*(3), 527-535. https://doi.org/10.17503/agrivita.v40i3.793

Nishida, S., Kato, A., Tsuzuki, C., Yoshida, J., & Mizuno, T. (2015). Induction of Nickel Accumulation in Response to Zinc Deficiency in *Arabidopsis thaliana*. *International Journal of Molecular Sciences*, *16*(5), 9420-9430. https://www.mdpi.com/1422-0067/16/5/9420

Nurzakiah, S., Sabiham, S., Nugroho, B., & Nursyamsi, D. (2014). Estimation of the potential carbon emission from acrotelmic and catotelmic peats. *Journal of Tropical Soils*, *19*(2), 81-89. https://doi.org/10.5400/jts.2014.v19i2.81-89

Nurzakiah, S., Wakhid, N., & Hairani, A. (2020). Carbon dioxide emission and peat hydrophobicity in tidal peatlands. *SAINS TANAH-Journal of Soil Science and Agroclimatology*, *17*(1), 71-77. https://doi.org/10.20961/stjssa.v17i1.41153

Olafisoye, O. B., Fatoki, O. S., Oguntibeju, O. O., & Osibote, O. A. (2020). Accumulation and risk assessment of metals in palm oil cultivated on contaminated oil palm plantation soils. *Toxicology Reports*, *7*, 324-334. https://doi.org/10.1016/j.toxrep.2020.01.016

Osakwe, S. A. (2013). Chemical partitioning of iron, cadmium, nickel and chromium in contaminated soils of south-eastern Nigeria. *Chemical Speciation & Bioavailability*, *25*(1), 71-78. https://doi.org/10.3184/095422913X13581872822530

Pulunggono, H. B., Anwar, S., Mulyanto, B., & Sabiham, S. (2019). Dinamika Hara Gambut Pada Penggunaan Lahan Hutan Sekunder, Semak Dan Kebun Kelapa Sawit. *Jurnal Pengelolaan Sumberdaya Alam dan Lingkungan (Journal of Natural Resources and Environmental Management)*, *9*(3), 692-699. https://doi.org/10.29244/jpsl.9.3.692-699

Pulunggono, H. B., Zulfajrin, M., & Hartono, A. (2020). Distribusi Sifat Kimia Gambut di Perkebunan Sawit dan Hubungannya dengan Kedalaman Lapisan Gambut dan Jarak dari Tanah Mineral Berbahan Induk Batuan Ultrabasa. *Jurnal Ilmu Tanah dan Lingkungan*, *22*(1). https://doi.org/10.29244/jitl.22.1.22-28

Rajapaksha, A. U., Vithanage, M., Oze, C., Bandara, W. M. A. T., & Weerasooriya, R. (2012). Nickel and manganese release in serpentine soil from the Ussangoda Ultramafic Complex, Sri Lanka. *Geoderma*, *189-190*, 1-9. https://doi.org/10.1016/j.geoderma.2012.04.019

Rinklebe, J., Antić-Mladenović, S., Frohne, T., Stärk, H.-J., Tomić, Z., & Ličina, V. (2016). Nickel in a serpentine-enriched Fluvisol: Redox affected dynamics and binding forms. *Geoderma*, *263*, 203-214. https://doi.org/10.1016/j.geoderma.2015.09.004

Rinklebe, J., & Shaheen, S. M. (2014). Assessing the Mobilization of Cadmium, Lead, and Nickel Using a Seven-Step Sequential Extraction Technique in Contaminated Floodplain Soil Profiles Along the Central Elbe River, Germany. *Water, Air, & Soil Pollution*, *225*(8), 2039. https://doi.org/10.1007/s11270-014-2039-1

Ritung, S., Suryani, E., Yatno, E., Hikmatullah, Nugroho, K., Sukarman, Subandiono, R. E., Hikmat, M., Tafakresnanto, C., Suratman, Hidayat, H., Sudrajat, D., Ponidi, Suryana, U., Supriatna, W., & Hartadi, A. (2019). *Indonesian Peatland Map, Scale 1:50.000 (Peta Lahan Gambut Indonesia Skala 1:50.000)*. Bogor, Indonesian Agency for Agricultural Research and Development (Balai Besar Penelitian dan Pengembangan Sumberdaya Lahan Pertanian). http://bbsdlp.litbang.pertanian.go.id/ind/index.php/publikasi/info-peta-gambut

Sabir, M., Hakeem, K. R., Aziz, T., Zia‐ur‐Rehman, M., Rashid, I., & Ozturk, M. (2014). High Ni levels in soil can modify growth performance and mineral status of wheat cultivars. *Clean–Soil, Air, Water*, *42*(9), 1263-1271.

Sangok, F. E., Sugiura, Y., Maie, N., Melling, L., Nakamura, T., Ikeya, K., & Watanabe, A. (2020). Variations in the rate of accumulation and chemical structure of soil organic matter in a coastal peatland in Sarawak, Malaysia. *CATENA*, *184*, 104244. https://doi.org/10.1016/j.catena.2019.104244

Sheng, G., Huang, C., Chen, G., Sheng, J., Ren, X., Hu, B., Ma, J., Wang, X., Huang, Y., Alsaedi, A., & Hayat, T. (2018). Adsorption and co-adsorption of graphene oxide and Ni(II) on iron oxides: A spectroscopic and microscopic investigation. *Environmental Pollution*, *233*, 125-131. https://doi.org/10.1016/j.envpol.2017.10.047

Sipos, P., Choi, C., Németh, T., Szalai, Z., & Póka, T. (2014). Relationship between iron and trace metal fractionation in soils. *Chemical Speciation & Bioavailability*, *26*(1), 21-30. https://doi.org/10.3184/095422914X13887685052506

Siqueira Freitas, D., Wurr Rodak, B., Rodrigues dos Reis, A., de Barros Reis, F., Soares de Carvalho, T., Schulze, J., Carbone Carneiro, M. A., & Guimarães Guilherme, L. R. (2018). Hidden Nickel Deficiency? Nickel Fertilization via Soil Improves Nitrogen Metabolism and Grain Yield in Soybean Genotypes [Original Research]. *Frontiers in Plant Science*, *9*(614). https://doi.org/10.3389/fpls.2018.00614

Sreekanth, T. V. M., Nagajyothi, P. C., Lee, K. D., & Prasad, T. N. V. K. V. (2013). Occurrence, physiological responses and toxicity of nickel in plants. *International Journal of Environmental Science and Technology*, *10*(5), 1129-1140. https://doi.org/10.1007/s13762-013-0245-9

Sutejo, Y., Saggaff, A., Rahayu, W., & Hanafiah. (2017). Physical and chemical characteristics of fibrous peat. AIP Conference Proceedings,

Takada, M., Shimada, S., & Takahashi, H. (2016). Tropical Peat Formation. In M. Osaki & N. Tsuji (Eds.), *Tropical Peatland Ecosystems* (pp. 127-135). Springer. https://doi.org/10.1007/978-4-431-55681-7_8

Tupaz, C. A. J., Watanabe, Y., Sanematsu, K., Echigo, T., Arcilla, C., & Ferrer, C. (2020). Ni-Co Mineralization in the Intex Laterite Deposit, Mindoro, Philippines. *Minerals*, *10*(7), 579. https://www.mdpi.com/2075-163X/10/7/579

Uruç Parlak, K. (2016). Effect of nickel on growth and biochemical characteristics of wheat (Triticum aestivum L.) seedlings. *NJAS - Wageningen Journal of Life Sciences*, *76*, 1-5. https://doi.org/10.1016/j.njas.2012.07.001

van der Ent, A., Echevarria, G., & Tibbett, M. (2016). Delimiting soil chemistry thresholds for nickel hyperaccumulator plants in Sabah (Malaysia). *Chemoecology*, *26*(2), 67-82. https://doi.org/10.1007/s00049-016-0209-x

Wakhid, N., Hirano, T., Okimoto, Y., Nurzakiah, S., & Nursyamsi, D. (2017). Soil carbon dioxide emissions from a rubber plantation on tropical peat. *Science of The Total Environment*, *581-582*, 857-865. https://doi.org/10.1016/j.scitotenv.2017.01.035

Wang, Y., Wang, S., Nan, Z., Ma, J., Zang, F., Chen, Y., Li, Y., & Zhang, Q. (2015). Effects of Ni stress on the uptake and translocation of Ni and other mineral nutrition elements in mature wheat grown in sierozems from northwest of China. *Environmental Science and Pollution Research*, *22*(24), 19756-19763. https://doi.org/10.1007/s11356-015-5153-8

Watanabe, T., Hasenaka, Y., Suwondo, Sabiham, S., & Funakawa, S. (2013). Mineral nutrient distributions in tropical peat soil of Riau, Indonesia with special reference to peat thickness. *Pedologist*, *57*(2), 64-71. https://doi.org/10.18920/pedologist.57.2_64

Yusuf, M., Fariduddin, Q., Hayat, S., & Ahmad, A. (2011). Nickel: An Overview of Uptake, Essentiality and Toxicity in Plants. *Bulletin of Environmental Contamination and Toxicology*, *86*(1), 1-17. https://doi.org/10.1007/s00128-010-0171-1

Yusuf, M., Fariduddin, Q., Varshney, P., & Ahmad, A. (2012). Salicylic acid minimizes nickel and/or salinity-induced toxicity in Indian mustard (*Brassica juncea*) through an improved antioxidant system. *Environmental Science and Pollution Research*, *19*(1), 8-18. https://doi.org/10.1007/s11356-011-0531-3

Zhang, X., Li, J., Wei, D., Li, B., & Ma, Y. (2015). Predicting Soluble Nickel in Soils Using Soil Properties and Total Nickel. *PLoS One*, *10*(7), e0133920. https://doi.org/10.1371/journal.pone.0133920

Zhang, Y., Qie, J., Wang, X. F., Cui, K., Fu, T., Wang, J., & Qi, Y. (2020). Mineralogical Characteristics of the Nickel Laterite, Southeast Ophiolite Belt, Sulawesi Island, Indonesia. *Mining, Metallurgy & Exploration*, *37*(1), 79-91. https://doi.org/10.1007/s42461-019-00147-y